108121-48-8; $Fe(PMe_3)_2(CNMe)_3$, 108121-41-1; $Fe(PMe_3)_2(CN\text{-}t\text{-}Bu)_3$, 108121-42-2; $Fe(PMe_3)(CN\text{-}t\text{-}Bu)_4$, 108121-46-6; $Fe(PMe_3)(CNCH_2CMe_3)_4$, 108121-47-7; $Fe(PMe_3)_3(CNCH_2CMe_3)_2$, 108121-49-9; $Fe(CN\text{-}t\text{-}Bu)_5$, 66415-98-3; $Fe(CNCH_2CMe_3)_5$, 108121-50-2; $FeCl_2$, 7758-94-3; t-BuNC, 7188-38-7; $CNCH_2CMe_3$, 72443-18-6.

Supplementary Material Available: For the four structure determinations, listings of bond distances and angles, fractional coordinates of placed hydrogen atoms, and anisotropic thermal parameters (27 pages); listings of calculated and observed structure factors (85 pages). Ordering information is given on any current masthead page.

Contribution from the Applied Sciences and Microgravity Section, Jet Propulsion Laboratory, California Institute of Technology, Pasadena, California 91109, and Inorganic and Structural Chemistry Group (INC-4) and Computing and Communication Division (C-8), Los Alamos National Laboratory, University of California, Los Alamos, New Mexico 87545

Assignment of the Rhodium–Rhodium Stretching Frequency in $Rh_2(O_2CCH_3)_4L_2$ Complexes and the Crystal and Molecular Structure of $[C(NH_2)_3]_2[Rh(O_2CCH_3)_4Cl_2]$. Relationship between Vibrational Spectra and Structure

Vincent M. Miskowski,*† Richard F. Dallinger,‡ Gary G. Christoph,§ David E. Morris,§ George H. Spies,∥ and William H. Woodruff*§

Received February 12, 1986

The resonance Raman spectra of salts of $[Rh_2(OAc)_4X_2]^{2-}$ (X = Cl^-, Br^-, I^-; OAc = O_2CCH_3) obtained by using ultraviolet laser excitation, and the structure of the salt $[C(NH_2)_3]_2[Rh_2(OAc)_4Cl_2]$, are reported. The salt crystallizes with two molecules per tetragonal (space group No. 87, $I4/m$) unit cell; a = 8.564 (1) Å and c = 13.955 (1) Å (T = −47 (1) °C). Least-squares refinement of 1395 unique reflections led to a final weighted $R(F^2)$ value of 0.053 ($R(F)$ = 0.030). Significant results of the structure determination are the Rh–Rh, Rh–Cl, and Rh–O distances of 2.3959 (3), 2.5853 (6), and 2.042 (1) Å, respectively. Ultraviolet resonance Raman results reveal that the rhodium–rhodium stretching motion of $[Rh_2(OAc)_4I_2]^{2-}$ is the predominant contributor to a normal vibrational mode observed at 314 cm^{-1}, rather than at 170 cm^{-1} as suggested in a previous assignment. In the bromide complex the analogous mode appears at 286 cm^{-1}. Simplified vibrational calculations yield a force constant of 2.60 mdyn/Å for the Rh–Rh bond in the iodide complex. This force constant is consistent with a new comprehensive relationship between force constants and bond distances, while a force constant based upon ν(Rh–Rh) ≈ 170 cm^{-1} is not.

Rhodium(II) acetate, $Rh_2(OAc)_4$, with its axial adducts and substituted carboxylate variants, is the prototypical example of a strong metal–metal single bond.[1] Yet, one of the most fundamental indicators of bond strength, the metal–metal stretching frequency (and the derived force constant of the Rh–Rh bond), has proved difficult to establish. Early Raman investigations of $Rh_2(OAc_2)_4L_2$ complexes, using laser excitation in the visible region of the spectrum, led to assignment of ν(Rh–Rh) to either of two polarized lines near 340 and 170 cm^{-1}.[2,3] The rationale for this assignment was largely that these were the strongest lines in the low-frequency Raman spectra. The 340-cm^{-1} assignment was recently eliminated by one of us,[4] who, with others, established that the 340-cm^{-1} vibration was clearly due to the totally symmetric ν[Rh–O(carboxylate)] stretching mode. The 170-cm^{-1} line could not be as thoroughly characterized at that time, and it was settled on as the "preferred" assignment, given the available possibilities. This assignment was nonetheless somewhat disturbing, as it implied[4] a large deviation from well-established empirical correlations (such as Badger's rule[5] and more recent relationships[6]) relating bond lengths and force constants for single metal–metal bonded compounds. Some reasons this might occur were suggested.[4] However, subsequent correlations[6] (vide infra) extending the empirical data to include all types and orders of bonding predict a symmetric Rh–O stretching frequency of 347 cm^{-1}, in good agreement with the Rh–O assignment noted above, but a Rh–Rh stretching frequency of 282 cm^{-1}. Clearly, the inconsistency of the ~170-cm^{-1} ν(Rh–Rh) assignment is too serious to be ignored. Either there is a complete breakdown in the general relationship between metal–metal bond length and stretching force constant for $Rh_2(OAc)_4$ or the assignment is wrong.

Our strategy in reexamining the Raman spectroscopy of $Rh_2(OAc)_4L_2$ was to choose complexes and laser excitation frequencies that offered the chance of lending strong resonance enhancement to vibrational modes containing large contributions from the Rh–Rh stretching coordinate. The $\sigma \rightarrow \sigma^*$ transitions directly involving the Rh–Rh bond are probably at too high energy to be near the frequency of available CW laser lines in the near-ultraviolet region (vide infra). Accordingly, we chose to tune the energy of the σ(Rh–L) → σ^*(Rh–Rh) transition, which should enhance both the Rh–L and Rh–Rh stretches, to be near our ultraviolet laser lines by judicious choice of the axial ligand L. Axial ligands examined included Cl^-, Br^-, I^-, and CH_3CN. The iodide complex proved to have its σ(Rh–L) → σ^*(Rh–Rh) transition close enough to laser lines near 350 nm to accomplish our objectives.

Reliable structural interpretation of the vibrational data requires knowledge of the structure of the specific salts involved. Because the solid-state spectra of the halide complexes examined in this study were taken on the guanidinium salts of $[Rh_2(OAc)_4X_2]^{2-}$, the crystal structure of the guanidinium salt of $[Rh_2(OAc)_4Cl_2]^{2-}$ was determined for comparison to existing structural data for $[Li(OH_2)_4X_2]$ salts in order to establish that the structural parameters of the $[Rh_2(OAc)_4X_2]^{2-}$ complex are not strongly dependent on counterion. The structural determination also serves to check the extraordinarily long Rh–Rh distance of 2.49 Å reported by Nefedor et al., as opposed to 2.397 Å found in the work cited above.[4] Such a variation is most unexpected from earlier work on these compounds and, if correct, would suggest that the Rh–Rh bond potential is very flat and the minimum easily influenced by the environment and nature of the counterions. This

* To whom correspondence should be addressed.
† California Institute of Technology.
‡ Department of Chemistry, Wabash College, Crawfordsville, IN 47933.
§ University of California.
∥ Present address: Department of Chemistry, Iowa State University, Ames, IA 50010.

(1) Cotton, F. A.; Walton, R. A. *Multiple Bonds between Metal Atoms*; Wiley-Interscience: New York, 1982.
(2) Ketteringham, A. P.; Oldham, C. *J. Chem. Soc., Dalton Trans.* **1973**, 1067.
(3) (a) Kharitonov, Y. Y.; Mazo, G. Y.; Knyazeva, N. A. *Russ. J. Inorg. Chem. (Engl. Transl.)* **1970**, *15*, 739–740. (b) San Filippo, J., Jr.; Sniadoch, H. J. *Inorg. Chem.* **1973**, *12*, 2326–2333.
(4) Miskowski, V. M.; Schaefer, W. P.; Sadeghi, B.; Santarsiero, B. D.; Gray, H. B. *Inorg. Chem.* **1984**, *23*, 1154–1162.
(5) (a) Badger, R. M. *J. Chem. Phys.* **1934**, *2*, 128; **1935**, *3*, 710. (b) Hershback, D. R.; Laurie, V. W. *J. Chem. Phys.* **1961**, *35*, 458.
(6) Woodruff, W. H., to be submitted for publication in *J. Am. Chem. Soc.*

0020-1669/87/1326-2127$01.50/0

Table I. Crystallographic Data for $[C(NH_2)_3]_2[Rh_2(OAc)_4Cl_2]$

Crystal Data
octahedral
prominent faces: (011), (101), 110
dimens: 0.24 mm along [110], r_{min} = 0.191 mm, r_{max} = 0.255 mm
transmission coefficients: max 0.764 (μ = 16.15 cm^{-1}, λ = 0.71069 Å), min 0.736
Data Collection
temp: −47 (1) °C (cold-gas-stream device)
cell constants: space group *I*4/*m* (No. 87), least-squares fit of setting angles for 43 reflecns having 17° < 2θ < 41°, a = 8.564 (1) Å, c = 13.955 (1) Å
wavelength: λ(Mo K$\bar{\alpha}$) = 0.71069 Å
density: measd (CCl_4/$CHBr_3$ flotation) 2.09 (2) g cm^{-3}, calcd (Z = 2) 2.058 g cm^{-3}
scan method: ω–2θ
scan rates: 2–24° min^{-1} (2θ)
scan width: 1.0° (2θ) below to 1.1° (2θ) above calcd Bragg, 2θ adjusted for wavelength dispersion
reflecns measd: 2531 with hkl > 0, 2θ ≤ 70.0°
unique reflecns: 1395
reflecns above 3σ: 1077
internal consistency of multiply measd reflecns:[a] $R'(F)$ = 0.015, $R'(wF^2)$ = 0.029

[a] Requirement:[11] full-matrix least squares on weighted F^2; $R(F)$ = 0.030 (1077 data), $R(wF^2)$ = 0.053 (1395 data), GOF = 1.45.

structural study was undertaken at about the same time as that of the lithium hydrated salt,[4] but independently.

The importance of $Rh_2(OAc)_4$ as a benchmark metal–metal-bonded complex was recently emphasized by a report[7] of a molecular mechanics calculation on $M_2(OAc)_4L_2$ and related complexes, which adopted the ~170-cm^{-1} ν(Rh–Rh) assignment. Interesting conclusions as to the importance of steric factors were arrived at in this study; but if the ν(Rh–Rh) assignment is uncertain, so are the conclusions. The present study is designed to resolve this question. Our results, along with resonance Raman results recently reported by Clark et al.,[24] provide convincing evidence that the correct frequency of ν(Rh–Rh) is indeed near the empirically predicted value of 282 cm^{-1}.

Experimental Section

Synthesis and Spectroscopy. The compounds $[Li(OH_2)_4]_2[Rh_2(OAc)_4Cl_2]$ and $Rh_2(OAc)_4(NCCH_3)_2$ were prepared by the method of ref 4, while the guanidinium salts, $[C(NH_2)_3]_2[Rh_2(OAc)_4X_2]$, X = Cl, Br, I, were prepared by the method of ref 9.

Raman spectra employed a Spex Ramalog EU spectrometer equipped with an ORTEC 9300 series photon-counting system and a Nicolet 1180E Raman data system. The 363.8-nm (Ar^+) and the 350.7-nm (Kr^+) lines of Spectra-Physics 171 ion lasers were used for excitation. All data were recorded at ~5 cm^{-1} spectral slit width. Solids were run as spinning KCl or KBr pellets.

X-ray Determination of the Structure of $[C(NH_2)_3]_2[Rh_2(OAc)_4Cl_2]$. Emerald green crystals of guanidinium tetrakis(μ-acetato)dirhodium dichloride were grown from an aqueous methanolic solution of dirhodium tetraacetate and guanidinium chloride. Systematic absences (hkl, $h + k + l = 2n + 1$) and apparent symmetry on preliminary precession photographs are consistent with several tetragonal space groups, viz., *I*4, $I\bar{4}$, and *I*4/*m* in particular, and several of higher symmetry. A small octahedral crystal with one apex truncated by the 110 face was used for all measurements, with the crystal mounted with the [101] direction roughly along the diffractometer ϕ axis. A Syntex P1 automated diffractometer employing graphite-monochromatized Mo Kα radiation was used for all measurements. The sample crystal was maintained at −47 (1) °C for cell constant and intensity collection by means of a flowing-cold-gas cooling device. Cell constants and other crystallographic data are summarized in Table I. Backgrounds were counted at each end of each scan for a total of half of the entire scan time. The intensities of 10 check reflections, widely dispersed in intensity and in reciprocal space, showed no significant systematic variation during the data collection. A total of 2531 reflections were measured, of which 1395 unique reflections remained after averaging of symmetry-equivalent (under 14) and multiply measured reflections. Absorption corrections (Gaussian integration using an 8×8×8 grid) left the R' factors (internal data agreement indices) essentially unchanged.

Assuming space group *I*4, to permit undisordered guanidinium groups, the structure was solved by the heavy-atom Patterson method. Refinement with all non-hydrogen atoms of the $[Rh_2(O_2CCH_3)_4Cl_2]^{2-}$ anion gave an $R(F)$ value of 0.16; however, the atom parameter shifts were highly correlated. A Fourier difference map revealed a highly disordered guanidinium ion located about ($^1/_2$, 0, $^1/_4$). The disorder was such that the apparent space group symmetry was *I*4/*m* (No. 87), and the refinement was accordingly continued in this higher symmetry space group, with the guanidinium carbon atom constrained to the special position and the partial nitrogen atoms at sites found on the difference map. Methyl hydrogen atoms on the anion were located from difference Fourier maps, and it was necessary to free the quanidinium group from the special position to continue the refinement. As the methyl hydrogen atoms refined to unrealistic positions, they were held fixed in essentially idealized geometry with the C–H distance set to 1.0 Å. As the guanidinium group(s) appeared highly distorted because of the disorder, no guanidinium hydrogen atoms were included in any of the calculations. More sophisticated attempts to model the guanidinium group proved unsuccessful. The final least-squares refinement (all shifts ≤0.1), with the inclusion of a secondary extinction correction,[10] gave $R(F)$ = 0.030, $R(wF^2)$ = 0.053, and GOF = 1.45.[11] Atomic scattering factors were

Table II. Final Values of Least-Squares Parameters for $[C(NH_2)_3]_2[Rh_2(OAc)_4Cl_2]$

	x	y	z	B,[a] Å^2
Rh	0	0	0.08584 (1)	1.621 (1)
Cl	0	0	0.27111 (4)	1.967 (4)
O	0.2093 (1)	0.1138 (1)	0.8053 (7)	2.33 (2)
C1	0.2695 (2)	0.1446 (2)	0	2.04 (2)
C2	0.4262 (3)	0.2241 (3)	0	2.86 (3)
N1	0.6100 (5)	0.1273 (4)	0.2151 (3)	4.51 (7)
N2	0.533 (2)	−0.1128 (9)	0.2403 (7)	5.3 (2)
C3	0.53 (2)	−0.02 (2)	0.247 (2)	2.7 (4)
H1	0.5199	0.1515	0	4.0
H2	0.4325	0.2906	0.0574	4.0

[a] B_{eq} = $8\pi^2U_{eq}$, where U_{eq} = $^1/_3\sum_i\sum_j(U_{ij}(a_i^*a_j^*)$; secondary extinction coefficient g = 0.52 (5) × 10^{-6}.[10]

Table III. Bond Distances (Å) and Angles (deg) for $[C(NH_2)_3]_2[Rh_2(OAc)_4Cl_2]$

Rh–Rh	2.3959 (3)	C2–C2	1.505 (3)
Rh–Cl	2.5853 (6)	N1–C3	1.52 (14), 1.21 (13)[a]
Rh–O	2.042 (1)	Nj2–C3	1.26 (15), 1.31 (14)[a]
C1–O	1.264 (1)		
Rh′–Rh–O	87.92 (3)	O′–C1–O	125.5 (2)
Rh–O–C1	119.3 (1)	O–C1–C2	117.2 (1)

[a] The guanidinium group is disordered with at least four orientations of the trigonal cation superimposed at the 4/*m* site. Selection of an appropriate set of symmetry-transformed coordinates for N1, N2, and C3 yields a reasonably flat, trigonal guanidinium group. The C3–C3′ distances range from 0.50 to 0.70 Å across the fourfold axis and mirror, respectively.

(7) Boeyens, J. C. A.; Cotton, F. A.; Han, S. *Inorg. Chem.* **1985**, *24*, 1750–1753.
(8) Nefedor, V. I.; Salyn, Ya. V.; Sadorskiy, A. P. *J. Electron Spectrosc. Relat. Phenom.* **1979**, *16*, 299.
(9) Nazarova, L. A.; Chernyaev, I. I.; Morozova, A. S. *Russ. J. Inorg. Chem.* (*Engl. Transl.*) **1966**, *11*, 1387–1389.
(10) Larson, A. C. *Acta Crystallogr.* **1967**, *23*, 664–665.
(11) The R' factors between multiply measured reflections were

$$R'(F) = (\sum_{hkl}\sum_{j=1}^{n}(|F_{av}| - |F_j|))/\sum_{hkl}nF_{av}$$

$$R'(wF^2) = ((\sum_{hkl}\sum_{j=1}^{n}w_j(F_{av}^2 - F_j^2)^2)/\sum_{hkl}\sum_{j=1}^{n}w_jF_{av}^4)^{1/2}$$

where w is the weight ($-1/\sigma^2(F^2)$) calculated for each ($F_{av}^2 - F_j^2$) including the covariance terms. The function minimized in the least squares was $\sum w(F_o^2 - F_c^2)^2$, where $w = \sigma^2(F_o^2)$. $R(F) = \sum||F_o| - |F_c||/\sum|F_o|$, $R(wF^2) = [\sum w(F_o^2 - F_c^2)^2/\sum wF_o^4]^{1/2}$, and GOF = $[\sum w(F_o^2 - F_c^2)^2/(n_{observn} - n_{param})]^{1/2}$. The CRYm crystallographic computing system (DuChamp, D. J. *Program and Abstracts*, American Crystallographic Association Meeting, Bozeman, MT, 1965; American Crystallographic Association: Storrs, CT, 1965; Paper B14) was used for all calculations.

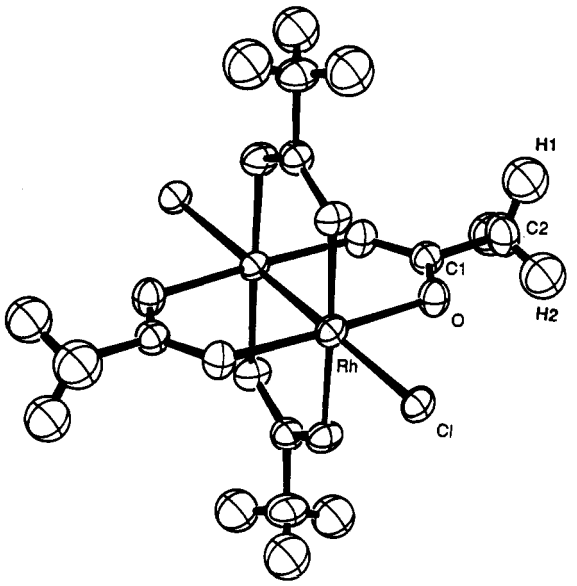

Figure 1. ORTEP drawing of the $[Rh_2(OAc)_4Cl_2]^{2-}$ structure in $[C(NH_2)_3]_2[Rh_2(OAc)_4Cl_2]$.

taken from the standard source,[12] except for that for hydrogen.[13] Final values of the least-squares-refined parameters are given in Table II and the derived bond distances and angles in Table III. The final difference Fourier map shows one large well-formed peak (0.8 e $Å^{-3}$), at the midpoint of the C–C bond; the next largest peak (0.6 e $Å^{-3}$) is at the rhodium position. Remarkably, the region about the guanidinium ion is featureless. The average noise level of the map is ±0.3 e $Å^{-3}$. Anisotropic thermal parameters and observed and calculated structure factor amplitudes are reported in the supplementary material.

Results and Discussion

Description of the Structure of $[C(NH_2)_3]_2[Rh_2(OAc)_4Cl_2]$. An ORTEP drawing of the structure of the $[Rh_2(OAc)_4Cl_2]^{2-}$ structural unit is shown in Figure 1. The Rh–Rh and Rh–Cl distances are 2.3959 (3) and 2.5853 (6) Å, respectively. These compare very well with the values found earlier for the same anion in $Li_2Rh_2(O_2CCH_3)_4Cl_2 \cdot 8H_2O$ of 2.397 (1) and 2.601 (1) Å. The nearly identical distances in these two studies show that the packing environment and the counterions do not seriously affect the Rh–Rh or Rh–Cl bond potentials, and this lends further credence to our interpretation of the vibrational spectra. Each rhodium atom is displaced 0.074 (2) Å outward from the plane of its four acetate oxygen ligands. The geometry of the bridging acetate framework is virtually identical with that of the bis(pyridine) adduct of this nucleus,[14] except that here rigorous $4/m$ symmetry is imposed by the space group symmetry; the Cl–Rh–Rh–Cl array is precisely linear. The guanidinium C–N distances and angles are very unreliable but surprisingly reasonable (compared to expected C–N = 1.217 (4) Å[15]) considering the extent of the disorder. The reason for the disorder is clear from the figures in the supplementary material, which show the likely hydrogen bonding between the ligand chloride and the surrounding disordered guanidinium cations. The cations are simultaneously involved in hydrogen bonding to neighboring chlorides, which give a fourfold symmetric electrostatic potential, and the trigonal cations are free to adopt any of a number of energetically equivalent positions about that site. The apparent N···Cl distances range from 3.33 to 3.60 Å. There are, in addition, four N···O contacts ranging from 3.10 to 3.19 Å.

Table IV. Low-Frequency Raman Spectra for $Rh_2(OAc)_4L_2$ Complexes with 363.8-nm Excitation

L	CH_3CN^a	OH_2^b	Cl^{-c}	Cl^{-d}	$Br^{-d,e}$	I^{-d}	I^{-f}
ν_s(Rh–O)	344	342	342	342	338	337	338
ν_{as}(Rh–O)	325	320	323	325	319	...[i]	...
ν(Rh–Rh)	...	...	...	...	286	314	314
δ(Rh–O)	170 (sh)	160 (sh)	170	170	170	...	...
ν_s(Rh–L)	...	...	...	...	118	91	88
ν_{as}(Rh–L)[g]	...	...	...	170	112	92[h]	...

[a] CH_3CN solution. [b] H_2O solution. [c] Solid, Li^+ salt. [d] Guanidinium salt. [e] 350.7-nm excitation, KBr pellet. [f] 50% saturated NaI solution. [g] IR values from ref 17. [h] Value for $K_2[Rh_2(O_2CH)_4I_2] \cdot H_2O$. [i] All entries marked with dots were not observed.

Since the dirhodium nucleus in this salt is virtually identical in structure with that of the bright red bis(pyridine) complex ($\lambda_{max} \approx 500$ nm), yet is green ($\lambda_{max} \approx 600$ nm) like the diaquo complex, we must look to factors other than the Rh–Rh bond strength/length as an indicator of the electronic levels involved in these visible transitions.

Spectroscopy and Assignments. We employed two simultaneous strategies in our efforts to establish ν(Rh–Rh) for $Rh_2(OAc)_4L_2$ complexes. First, we looked at the series of axial adducts $Rh_2(OAc)_4X_2^{2-}$, X = Cl, Br, I, following the established principle[16] that mass (kinematic) effects of the axial ligand along this series should introduce predictable variations in ν(Rh–Rh). Second, we employed UV (363.8 and 350.7 nm) excitation. Since intense electronic absorption transitions involving population of the Rh–Rh $d\sigma^*$ level are in the UV region,[4] we hoped that axial modes (ν(M–M), ν(M–X)) would be selectively intensified.

The Raman spectra of $Rh_2(OAc)_4(NCCH_3)_2$, and also the guanidinium salts of $Rh_2(OAc)_4X_2^{2-}$, are shown in Figure 2 and summarized in Table IV, as obtained with UV excitation. In the chloride and bromide complexes, we see lines at about 340, 325, and 170 cm^{-1}, which are totally independent of axial ligand. The first two of these lines have been assigned[4] to totally symmetric and non totally symmetric ν[Rh–O(carboxylate)] modes, respectively, and the axial ligand independence of our present results supports these assignments. We have determined depolarization ratios for the bis(acetonitrile) complex for 363.8-nm excitation (Figure 3). Just as for visible excitation,[4] the 322-cm^{-1} line is depolarized while the 344-cm^{-1} line is strongly polarized. The spectrum of the $Li(OH_2)_4^+$ salt of $[Rh_2(OAc)_4Cl_2]^{2-}$ was identical to that of the guanidinium salt (Table IV).

It is important that the 170-cm^{-1} line is also independent of axial ligand. If this line were really the ν(Rh–Rh) mode, mass effects should have caused it to shift along the halide series. Far-infrared results[17] place the A_{2u} ν(Rh–X) band at low frequency (170 cm^{-1} for $[C(NH_2)_3]_2[Rh_2(OAc)_4Cl_2]$, 112 cm^{-1} for $[C(NH_2)_3]_2[Rh_2(OAc)_4Br_2]$), and the A_{1g} ν(Rh–X) modes should have similar frequencies; thus, mixing between a 170-cm^{-1} ν(Rh–Rh) band and ν(Rh–X) should unquestionably have caused ν(Rh–Rh) to vary, by both **G** and **F** matrix mixing.

Figure 4 shows the empirical relationship[6] between force constants and bond distances for bonding between elements in the row of the periodic table containing rhodium and the second transition series. This plot includes *all* bonded systems within this row for which (a) the bond distances are known and (b) the force constants of the bonds are known from vibrational analysis or can be reliably estimated by the diatomic approximation or from compressibility measurements. All conceivable types of bonding are included: solid metals, "ionic" solids, gas-phase diatomics, metal–metal-bonded systems with and without bridging ligands and with bond orders ranging from formally zero (d^8 dimers) to four or greater ($Mo_2(g)$), homonuclear and heteronuclear bonding involving main-group and transition elements,

(12) *International Tables for X-ray Crystallography*; Kynoch: Birmingham, England, 1962; Vol. III, pp 202–203.
(13) Stewart, R. F.; Davidson, E. R.; Simpson, W. T. *J. Chem. Phys.* **1965**, *42*, 3175–3187.
(14) Koh, Y. B.; Christoph, G. G. *Inorg. Chem.* **1978**, *17*, 2590.
(15) Morimoto, C. N.; Lingafelter, E. C. *Acta Crystallogr., Sect. B: Struct. Crystallogr. Cryst. Chem.* **1970**, *B26*, 335–341.
(16) (a) Stein, P.; Dickson, M. K.; Roundhill, D. M. *J. Am. Chem. Soc.* **1983**, *105*, 3489–3494. (b) Miskowski, V. M.; Smith, T. P.; Loehr, T. M.; Gray, H. B. *J. Am. Chem. Soc.* **1985**, *107*, 7925–7934.
(17) Mazo, G. Y.; Baranovskii, I. B.; Shchelokov, R. N. *Russ. J. Inorg. Chem. (Engl. Transl.)* **1979**, *24*, 1855.

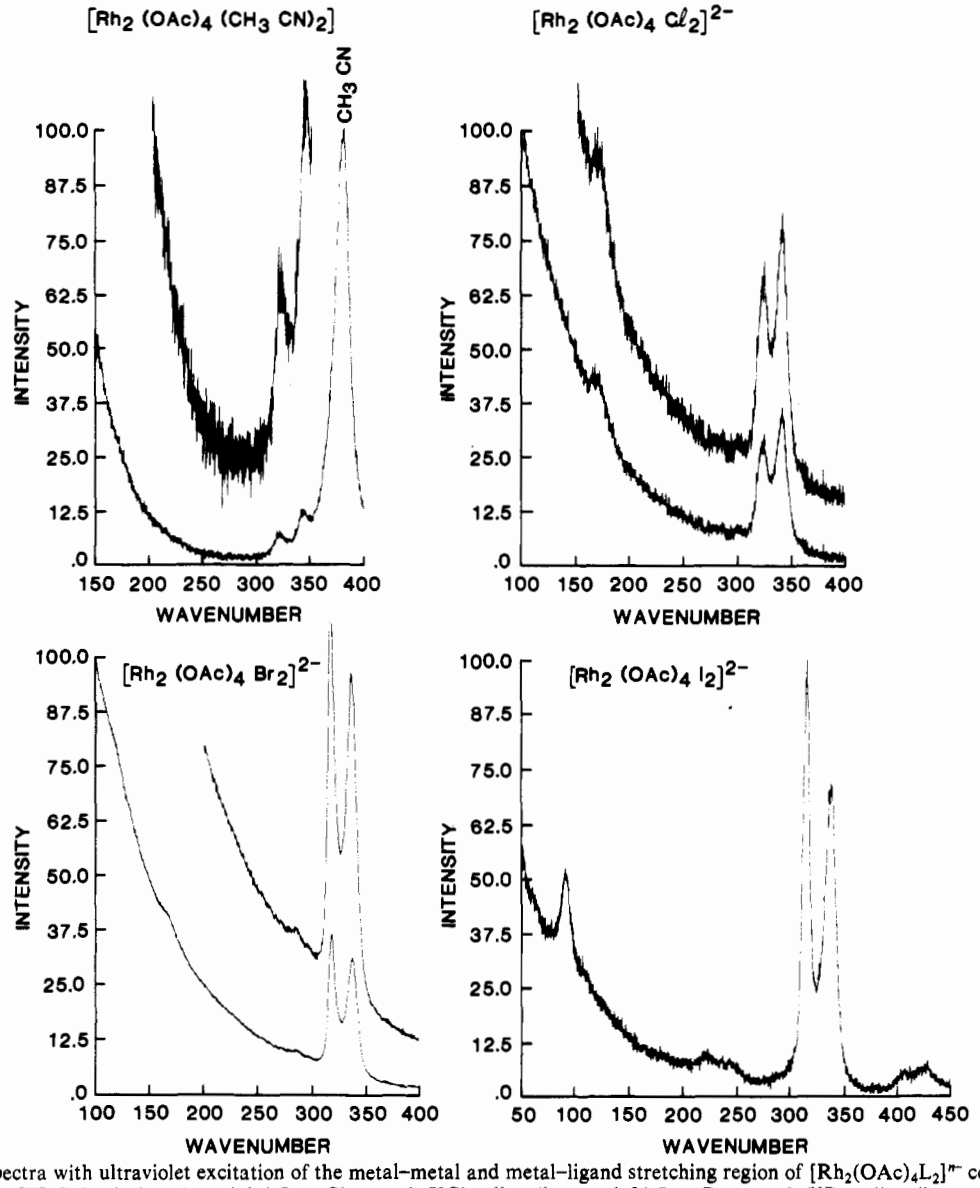

Figure 2. Raman spectra with ultraviolet excitation of the metal–metal and metal–ligand stretching region of $[Rh_2(OAc)_4L_2]^{n-}$ complexes: (top left) L = CH_3CN, n = 0, CH_3CN solution; (top right) L = Cl^-, n = 2, KCl pellet; (bottom left) L = Br^-, n = 2, KBr pellet; (bottom right) L = I^-, n = 2, KCl pellet.

ground and excited electronic states, etc. The only significant deviations from this correlation occur for extremely weak bonding (force constants less than 0.1 mdyn/Å, bond distances greater than ~3.35 Å) and solid metals having the ccp structure. The exponential decay function

$$r\ (\text{Å}) = 1.83 + 1.51[\exp(-F/2.48)]$$

where r is the internuclear distance and F is the force constant in mdyn/Å, fits the experimental data with a standard deviation in r of ±0.03 Å. Clearly, a major deviation from this correlation for the Rh–Rh bond in $Rh_2(OAc)_4$ is not to be expected. Using this function and the crystallographically determined Rh–Rh distance leads to a predicted frequency for the Rh–Rh stretch of 282 cm^{-1} (diatomic approximation). The asterisk on the plot represents the position of the $Rh_2(OAc)_4$ point if the 170-cm^{-1} mode were indeed the Rh–Rh stretch. This point falls off of the empirical correlation function by 0.5 Å or 17σ! At the same time, the frequency predicted for the symmetric Rh–O stretch by using functions of this type for the first row of the periodic table and interrow bonding[6] is 347 cm^{-1}, to be compared to the observed value[4] of 342 cm^{-1}.

We conclude that the 170-cm^{-1} mode is *not* ν(Rh–Rh); the likely correct assignment of this feature is to the totally symmetric O–Rh–Rh deformation, δ(Rh–O), which has been placed in this frequency region by a previous study[18] of metal carboxylate complexes.

Where are the axial modes? Some evidence concerning this question comes from our study of the bromide complex, wherein we do see two additional weak features in the spectrum, at 118 and 286 cm^{-1}. The former is likely to be ν(Rh–Br), by comparison to the IR (A_{2u}) ν(Rh–Br) frequency[19] of 112 cm^{-1}. The latter may be the Rh–Rh stretch. Much stronger evidence comes from our RR results on the $Rh_2(OAc)_4I_2^{2-}$ ion, which we have studied both in solution (50% standard KI(aq)) and as the guanidinium salt diluted into a KCl pellet. Previous work[4] indicates that 363.8-nm excitation should be near resonance with a very intense σ(Rh–I) → σ^*(Rh–Rh) transition (λ_{max} = 332 nm, ϵ = 27 000) for this complex, and we accordingly observe (Figure 5) both enormously increased Raman scattering for this complex and, characteristic of resonance, overtones and combinations.

There are four lines attributable to fundamental modes: 91, 314, 337, and 727 cm^{-1}. The last of these is probably the symmetric CO_2 angle bend of the bridging acetate; since combinations

(18) Bratton, W. K.; Cotton, R. A.; DeBeau, M.; Walton, R. A. *J. Coord. Chem.* **1971**, *1*, 121–131.
(19) Koh, Y. B.; Christoph, G. G. *Inorg. Chem.* **1979**, *18*, 1122–1128.

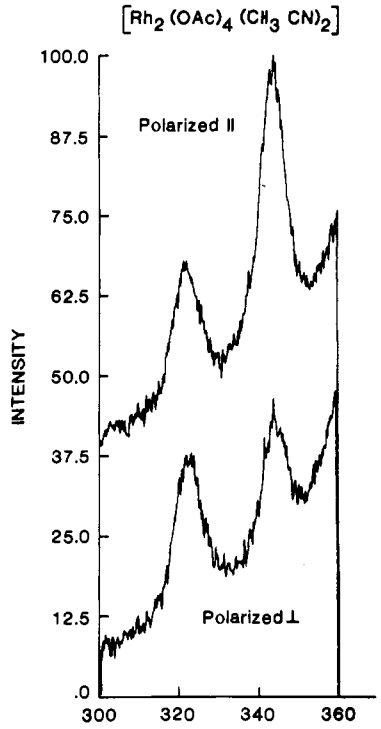

Figure 3. Polarized Raman spectra of the 300–360-cm^{-1} region of $Rh_2(OAc)_4(CH_3CN)_2$ in CH_3CN solution: (top) parallel polarization; (bottom) perpendicular polarization.

of it with the 314/337-cm^{-1} lines are observed, it also appears to be resonance-enhanced, which can be understood on the basis that structural compilations[19] indicate the O–C–O angle to be sensitive to metal–metal distance. The 91-cm^{-1} line is assigned to ν(Rh–I) and may be compared to 92 cm^{-1} reported[17] for the A_{2u} ν(Rh–I) band of the compound $K_2[Rh_2(O_2CH)_4I_2]H_2O$. With regard to the combination involving the 91-cm^{-1} mode, at room temperature 40% of the molecules should be thermally excited by one quantum of this mode; thus, observation of peaks due to difference combinations (e.g., those at 222 and 245 cm^{-1}) with nearly as much intensity as the positive combinations (those at 408 and 427 cm^{-1}) is understandable. The difference modes should, of course, lose intensity as temperature is lowered.

We determined depolarization ratios for a solution in 50% saturated NaI(aq) under N_2; the high I^- concentration is necessary to ensure complete formation of the diiodide complex. As shown in Figure 6, the lines at 314 and 338 cm^{-1} are both strongly polarized,[20] $\rho \approx 0.2$, indicating them to be totally symmetric modes. The 314-cm^{-1} line is, therefore, *not* a non totally symmetric ν(Rh–O) mode analogous to the ~325-cm^{-1} line[4] observed in the other complexes when either visible or ultraviolet excitation is used.

We suggest that the 314-cm^{-1} line is the rhodium–rhodium stretch, ν(Rh–Rh). In resonance with the σ(Rh–I) → σ^*(Rh–Rh) transition, the symmetric ν(Rh–Rh), ν(Rh–O), and ν(Rh–I) modes have all been enormously intensified,[21] while the unobserved δ(Rh–O) and ν_{as}(Rh–O) modes are not resonance-enhanced.

We similarly propose that weak preresonance with σ(Rh–Br) → σ^*(Rh–Rh) (λ_{max} = 291 nm)[4] accounts for the slight intensity seen for ν(Rh–Br) at 118 cm^{-1} in $[Rh_2(OAc)_4Br_2]^{2-}$; we further suggest that the weak 286-cm^{-1} line is ν(Rh–Rh) for this complex. For the other complexes, intense axial electronic transitions are all at considerably higher energy;[4] the low-lying electronic transitions are all essentially equatorial excitations, which accounts for the vanishingly small intensity seen for the axial modes.

A linear I–Rh–Rh–I force field calculated[16] by using our assignments for the axial modes produces a solution of 2.60 mdyn/Å for the rhodium–rhodium force constant (0.71 mdyn/Å for k(Rh–I)). This value corresponds to a "bare" $Rh_2(OAc)_4$ ν(Rh–Rh) frequency of 293 cm^{-1}, which, in turn, compares favorably with the frequency of 282 cm^{-1} predicted empirically from the crystallographic Rh–Rh distance (vide supra). That this frequency is lower than the experimental $Rh_2(OAc)_4I_2^{2-}$ value is a result of kinematic interaction with the very heavy iodide ligands.[22]

We would, therefore, expect complexes such as $Rh_2(OAc)_4(OH_2)_2$ with light axial ligands to show ν(Rh–Rh) near[23] 280–300

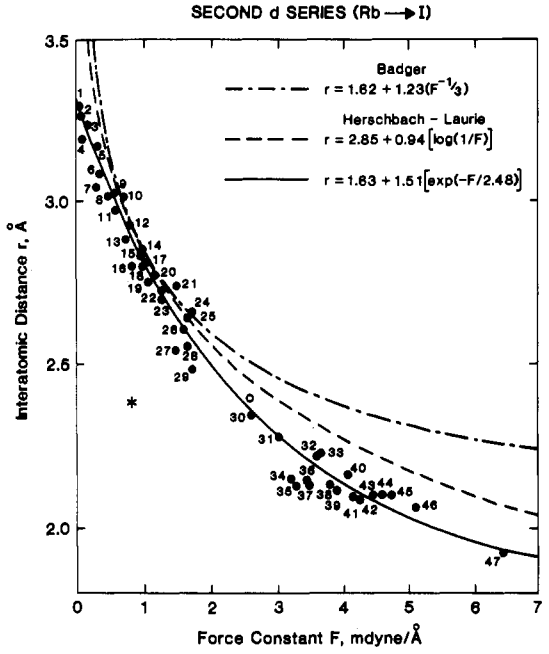

Figure 4. Plot of force constant vs. bond distance for bonds between elements of the row of the periodic table from Rb through I. The asterisk represents the point for a $Rh_2(OAc)_4$ unit having a Rh–Rh distance of 2.396 Å and ν(Rh–Rh) = 170 cm^{-1} (diatomic approximation for force constant). The open circle is the $Rh_2(OAc)_4$ point if the force constant is 2.60 mdyn/Å. The dashed lines are from ref 5. The solid line is the function from the present work, to be discussed in detail elsewhere.[6] Identity of points: (1) Cd metal; (2) Rh_2(2,5-diisocyano-2,5-dimethylhexane)$_4^{2+}$; (3) $Rh_2[CN(CH_2)_3NC]_4^{2+}$; (4) $[Rh(CNC_6H_5)_4]_2^{2+}$; (5) Sn metal; (6) RbI(g); (7) Zr metal; (8) Sn′ metal; (9) I_2(g) ($^3\Pi$); (10) $Tc_2(CO)_{10}$; (11) Cd′ metal; (12) I_3^-; (13) Te_2(g) (O_u^+); (14) $[Rh_2[CN(CH_2)_3NC]_4Cl_2]^{2+}$; (15) $Ru_3(CO)_{12}$; (16) CdTe(s); (17) Te_2(g) ($^3\Sigma_u^-$); (18) Sn(s, diamond); (19) InI(g) ($^1\Sigma^+$); (20) $[Rh_2$(2,5-diisocyano-2,5-dimethylhexane)$_4Cl_2]^{2+}$; (21) InI_3; (22) SbI_3; (23) Mo metal; (24) SnI_4; (25) I_2(g) ($^1\Sigma_g^+$); (26) $Mo_6Cl_{14}^{2-}$; (27) AgI(g) ($^1\Sigma^+$); (28) CdI_2; (29) Sb_2(g) (O_u^+); (30) Sb_2(g) ($^1\Sigma_g^+$); (31) $Ru(O_2CR)_4$; (32) $[Mo_2(HPO_4)_4{\cdot}2H_2O]^{2-}$; (33) $[Mo_2(HPO_4)_4{\cdot}Cl](Hpy)_3$; (34) $[Mo_2(CH_3)_8]^{4-}$; (35) $Mo_2I_4(PR_3)_4$; (36) $[Mo_2Cl_8]^{4-}$; (37) $Mo_2Cl_4(PR_3)_4$, $Mo_2Br_4(PR_3)_4$; (38) $Mo_2(O_2CCF_3)_4{\cdot}2py$; (39) $[Mo_2(SO_4)_4]^{4-}$; (40) $[Mo_2(SO_4)_4]^{3-}$, $Ru_2(O_2CCH_3)_4Cl$; (41) $Mo_2Br_2(O_2C_6H_5)_2(PR_3)_2$; (42) $Mo_2[(CH_2)_2P(CH_3)_2]_4$; (43) $Mo_2(O_2CCF_3)_4$; (44) $Mo_2(O_2CR)_4$; (45) $Mo_2[C_6H_5C(NC_6H_5)_2]_4$; (46) Mo_2(2-methyl-6-oxopyridine)$_4$; (47) Mo_2(g) ($^1\Sigma_g^+$).

(20) We have not studied the frequency dispersion of the depolarization ratios, varying excitation frequency, so the significance of the observed values (roughly intermediate between those expected[4] for purely axial or equatorial modes) is not clear.

(21) That the RR intensity of ν(Rh–I) is relatively smaller than that of ν_2 and ν_3 is not inconsistent with the I^- to $Rh_2(\sigma^*)$ charge-transfer electronic transition assignment, as ν(Rh–I) is a much lower frequency, hence high amplitude, vibration; the major excited-state distortion is indeed indicated to be along the Rh–I coordinate. The considerable RR intensity for ν_3, the Rh–O stretch, is a little surprising, however, as a first approximation Rh–O bonding should be unaffected by the electronic transition. We suspect that the very close proximity of ν_2 and ν_3 has resulted in some mixing of their vibrational coordinates, e.g., that ν_3 has some ν(Rh–Rh) character.

(22) For light axial ligands, a linear force field yields a familiar prediction of values of ν(Rh–Rh) lower than the bare Rh_2 value for a given F(Rh–Rh), corresponding to larger effective mass of the "diatomic" (LRh_2) oscillator. However, for very heavy axial ligands, ν(Rh–Rh) is predicted to be greater than the bare value by the factor $[1 + [F(Rh–Rh)/2F(Rh–Rh)]]^{1/2}$ for an infinitely heavy axial ligand. We have too little information available to calculate realistic force fields, but it seems likely that $Rh_2(OAc)_4L_2$ compounds for which ν(Rh–Rh) values are now available (this work and ref 24) fall in the heavy-axial-ligand regime.

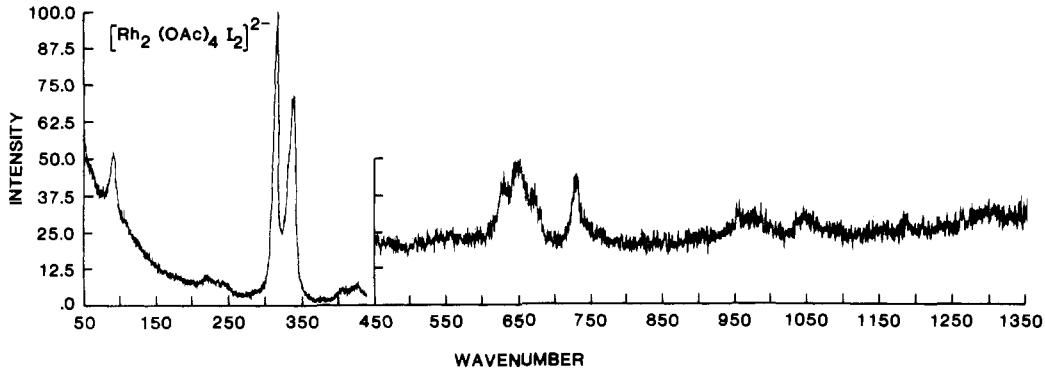

Figure 5. Resonance Raman spectrum with ultraviolet excitation of $[Rh_2(OAc)_4I_2]^{2-}$, showing the overtone and combination regions of the spectrum as well as the fundamentals.

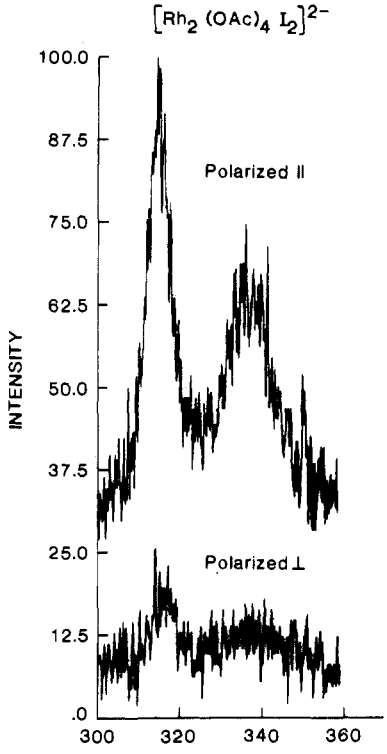

Figure 6. Polarized resonance Raman spectra of the 300–360-cm^{-1} region for $[Rh_2(OAc)_4I_2]^{2-}$ in a 50% saturated aqueous solution of NaI: (top) parallel polarization; (bottom) perpendicular polarization.

cm^{-1}. This value is in accord with the empirical prediction[6] and the above vibrational analysis of the I–Rh–Rh–I structure. We note that the Raman spectrum of, for example, $Rh_2(OAc)_4(CH_3OH)_2$ does show very weak lines near 300, 294, and 310 cm^{-1} according to ref 3b, but conclusive identification of these modes is not possible without isotope-substitution data.

(23) In an excited state involving population of σ^*(Rh–Rh), the metal–metal distance should be considerably longer and ν(Rh–Rh) considerably lower than for the ground state; this accounts for the resonance enhancement of ν(Rh–Rh) by the σ(Rh–X) → σ^*(Rh–Rh) electronic transition. We note that an ~300-cm^{-1} vibronic interval seen in the visible electronic absorption bands of $Rh_2(OAc)_4L_2$ compounds[4] is *not* attributable to ν(Rh–Rh) and does *not* support assignments of the transitions to σ^*(Rh–Rh), since the excited-state frequency is not much lower than the ground-state value of ν(Rh–Rh), as it would have to be for population of σ^*(Rh–Rh). The best interpretation of the vibronic structure remains that it is ν(Rh–O), reduced from the ground-state value as expected for σ^*(Rh–O) excited states.[4] The present recognition that visible excitation results in Raman activity of *only* the equatorial ν(Rh–O) and δ(Rh–O) modes is highly consistent with this interpretation.

Subsequent to completion of this work, we learned of work by Clark et al.[24] establishing assignment of a Raman line of $Rh_2(OAc)_4(P(C_6H_5)_3)_2$ at 289 cm^{-1} to ν(Rh–Rh). The Rh_2 bond length of this compound, 2.45 Å, should result in a bare ν(Rh–Rh) band about 5% lower than that of $Rh_2(OAc)_4Cl_2^{2-}$, or about 270 cm^{-1}. The higher value observed for the $P(C_6H_5)_3$ adduct (and also[24] for the As and Sb analogues) probably results from kinematic effects[22] involving the heavy axial ligands. Unfortunately, no information is available as to ν(Rh–L) stretching frequencies for these compounds. We note that the resonant electronic transition is probably σ(Rh–E) → σ^*(Rh–Rh) (E = P, As, Sb) rather than σ(Rh–Rh) → σ^*(Rh–Rh), following a previous line of argument,[4] so low-frequency ν(E–Rh) modes should be resonantly enhanced to some extent.[23]

In conclusion, we find that previous assignments of ν(Rh–Rh) for $Rh_2(OAc)_4L_2$ complexes are in error because ν(Rh–Rh) "accidentally" has very little Raman intensity, when visible laser excitation is used, due to a poor resonance condition for enhancement of the metal–metal stretch. This result emphasizes that assignment of low-frequency Raman modes must always take account of the possibility that resonance effects may lead to deceptive intensity ratios. Such difficulties can be overcome, as in the present study, by tuning both the exciting frequency *and* the absorption spectrum of the compound (as for the iodide axial adduct) so as to resonantly enhance the vibrational modes of interest in a predictable fashion. Our conclusions as to the identity of the ν(Rh–Rh) mode are in agreement with the assignment of Clark et al.[24] and with empirical predictions of the force constant associated with the Rh–Rh bond.[6]

Acknowledgment. This work was performed at Los Alamos National Laboratory under the auspices of the U.S. Department of Energy, at the Jet Propulsion Laboratory under the auspices of the National Aeronautics and Space Administration, and at the University of Texas at Austin under NSF Grant CHE 84-03836. We are grateful to Professor Robin Clark for helpful discussions and communication of results.

Registry No. $[C(NH_2)_3]_2[Rh_2(OAc)_4Cl_2]$, 36606-01-6; $[C(NH_2)_3]_2[Rh_2(OAc)_4Br_2]$, 36605-66-0; $[C(NH_2)_3]_2[Rh_2(OAc)_4I_2]$, 107202-72-2; $Rh_2(OAc)_4(NCCH_3)_2$, 80419-75-6; $[Li(OH_2)_4]_2[Rh_2(OAc)_4Cl_2]$, 88945-58-8; Rh, 7440-16-6.

Supplementary Material Available: For $[C(NH_2)_3]_2[Rh(O_2CCH_3)_4Cl_2]$, a table of anisotropic thermal parameters and Supplementary Figures 1–4 illustrating the network of hydrogen bonding between the chloride ligands and the guanidinium counterions (5 pages); a table of observed and calculated structure factor amplitudes (8 pages). Ordering information is given on any current masthead page.

(24) Clark, R. J. H.; Hempleman, A. J.; Flint, C. D. *J. Am. Chem. Soc.* **1986**, *108*, 518–520.